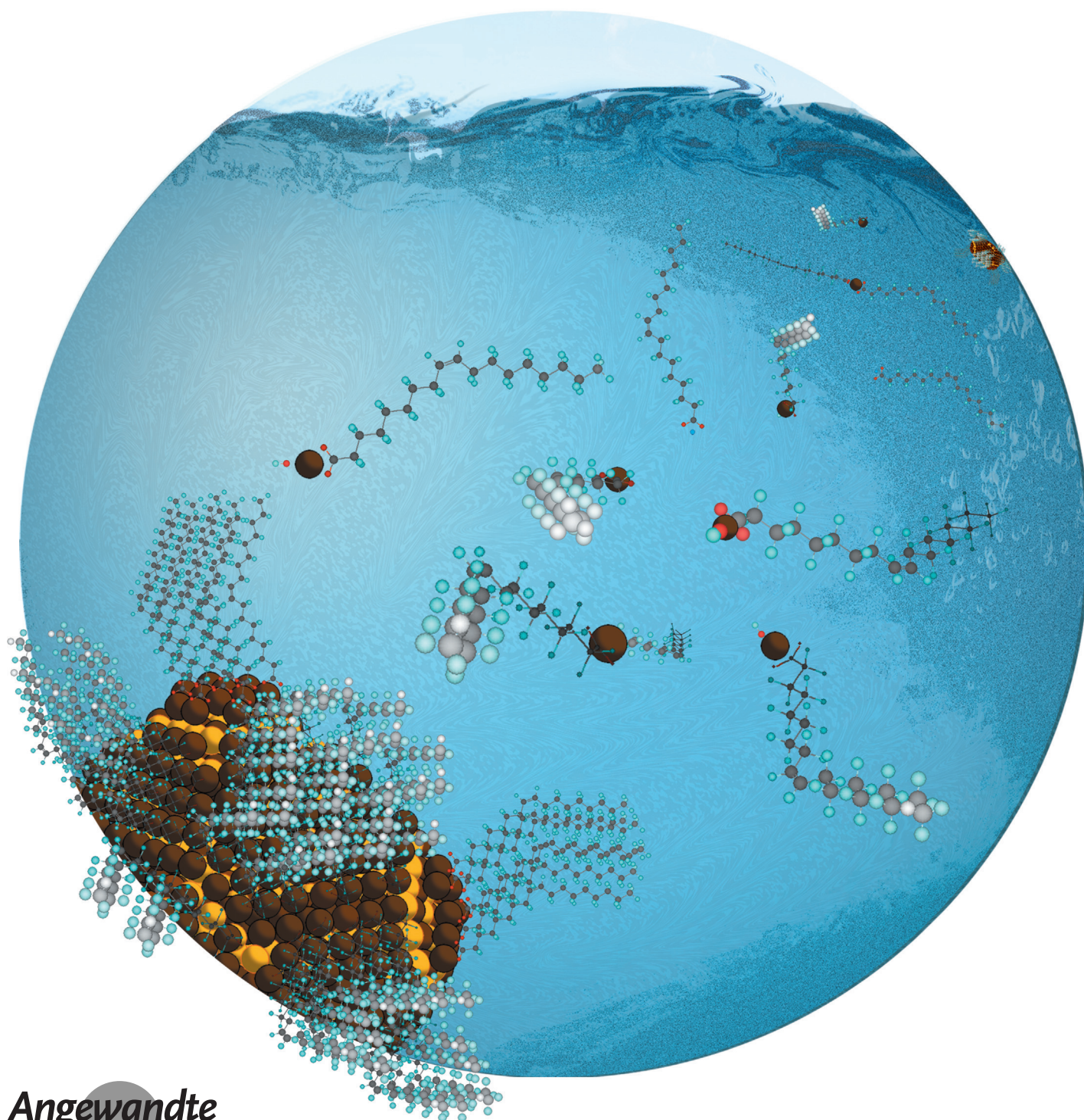


Quantum Dots

International Edition: DOI: 10.1002/anie.201511174
German Edition: DOI: 10.1002/ange.201511174

The Dynamic Organic/Inorganic Interface of Colloidal PbS Quantum Dots

Roberto Grisorio, Doriana Debellis, Gian Paolo Suranna, Giuseppe Gigli, and Carlo Giansante*



Abstract: Colloidal quantum dots are composed of nanometer-sized crystallites of inorganic semiconductor materials bearing organic molecules at their surface. The organic/inorganic interface markedly affects forms and functions of the quantum dots, therefore its description and control are important for effective application. Herein we demonstrate that archetypal colloidal PbS quantum dots adapt their interface to the surroundings, thus existing in solution phase as equilibrium mixtures with their (metal-)organic ligand and inorganic core components. The interfacial equilibria are dictated by solvent polarity and concentration, show striking size dependence (leading to more stable ligand/core adducts for larger quantum dots), and selectively involve nanocrystal facets. This notion of ligand/core dynamic equilibrium may open novel synthetic paths and refined nanocrystal surface-chemistry strategies.

As-synthesized colloidal quantum dots (QDs) are composed of nanometer-sized crystallites of inorganic semiconductor materials surrounded by organic molecules—and/or metal complexes—as ligands that coordinate the core surface preventing aggregation and ensuring solubility. The ligand/core (organic/inorganic) interface exerts a relevant role in the synthetic control of QD size and shape,^[1] markedly affects the electronic structure of colloidal QDs,^[2] and mediates QD non-covalent bonding interactions with other QDs or different chemical species.^[3] A thorough description of the organic/inorganic interface is therefore essential for the development of refined synthetic strategies^[4] and for the effective application of QDs in (opto)electronic devices and as luminescent materials,^[5] among others, to which aim metal chalcogenides are the most employed colloidal QD systems. Although frequently represented as discrete entities stably dispersed in a liquid phase, the static depiction of metal chalcogenide QDs and of their surface chemistry is fallacious: indeed, the QD growth mechanism implies a dynamic organic/inorganic interface at high temperatures,^[1] whereas the room-temperature effect of extra added Lewis bases has led to indirectly infer the lability of neutral ligands at the core surface, either as electron-donor organic species^[6] or as electron-acceptor

metal complexes.^[7] Herein we provide direct evidence that archetypal PbS QDs, synthesized according to the most widely employed procedure,^[8] exist in the solution phase as equilibrium mixtures with their ligand and core components in response to the QD's surroundings. Both organic molecules and metal complexes as ligands in mutual exchange are demonstrated to undergo dynamic equilibrium with the PbS core surface. Such interfacial equilibria depend on the solvent polarity and on QD concentration and size, prevalently involving specific nanocrystal facets.

We pursued a detailed compositional description of as-synthesized PbS QDs by elemental and thermogravimetric analysis (via inductively coupled plasma atomic emission spectroscopy and TGA, respectively) and by spectroscopic characterization (Fourier-transform infrared spectroscopy, FTIR, and NMR spectroscopy). We applied a standardized QD purification procedure to avoid the otherwise uncontrollable removal of Pb oleate and/or oleic acid ligands from the surface of the QDs.^[7,9] All the subtly purified QD samples show Pb-rich stoichiometries and bear one oleyl-based ligand per excess Pb atom, in agreement with previous observations on related QDs.^[10] The relationship between the amount of Pb, S, and oleyl moieties accounts for a QD structure consistent with an Archimedean truncated octahedron (compatible with the rock-salt crystal structure of PbS) completely terminated by Pb cations, which lay at the {111} facets and above every S anion of the {100} facets independently from the PbS core size (from ca. 2 to 7 nm). The corresponding ligand coverage (oleyl/nm²) increases with QD size, as a result of the proportionality between the surface-atom coverage of PbS crystallites and the core diameter ($N_{\text{surf}}/\text{nm}^2$) ascribable to Pb oleate ligands at the {100} facets (Figure 1; further details are given in Supporting Information).

The 1:1 ratio of oleyl-based ligands per excess Pb atoms (Pb_{exc}) poses questions as to how QD charge neutrality is preserved. Since the oxidation state of Pb atoms in QDs can safely be assumed to be 2+ derived from the Pb^{II}-oxide reagent, another anionic species is therefore expected to coordinate each Pb_{exc} . The FTIR spectra of the QDs in solid-phase indicate the presence of hydroxy groups at the QD surface (Figures 2a and Supporting Information) by showing

[*] Dr. C. Giansante

Center for Biomolecular Nanotechnologies @UNILE
Istituto Italiano di Tecnologia
Via Barsanti, 73010 Arnesano (Italy)
E-mail: carlo.giansante@iit.it

Dr. R. Grisorio, Prof. G. P. Suranna, Prof. G. Gigli, Dr. C. Giansante
CNR NANOTEC—Istituto di Nanotecnologia
Via Monteroni, 73100 Lecce (Italy)

Dr. R. Grisorio, Prof. G. P. Suranna
DICATECh—Dipartimento di Ingegneria Civile, Ambientale, del
Territorio, Edile e di Chimica, Politecnico di Bari
Via Orabona 4, 70125 Bari (Italy)

D. Debellis, Prof. G. Gigli, Dr. C. Giansante
Dipartimento di Matematica e Fisica “E. De Giorgi”
Università del Salento
Via per Arnesano, 73100 Lecce (Italy)
E-mail: carlo.giansante@unisalento.it

Supporting information and the ORCID identification number(s) for the author(s) of this article can be found under <http://dx.doi.org/10.1002/anie.201511174>.

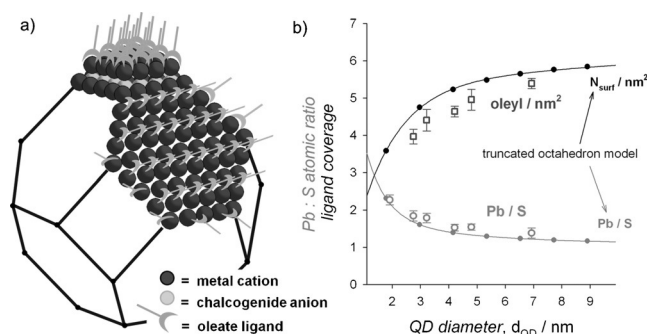


Figure 1. a) Depiction of the fully Pb-terminated truncated octahedral PbS QDs. b) Plots of the Pb/S atomic ratio (gray) and of the ligand coverage (oleyl/nm²; black) as function of QD size. Experimental data are given (open symbols) along with that for the truncated octahedron model (closed symbols; number of surface atoms per unit area at the QD surface, $N_{\text{surf}}/\text{nm}^2$).

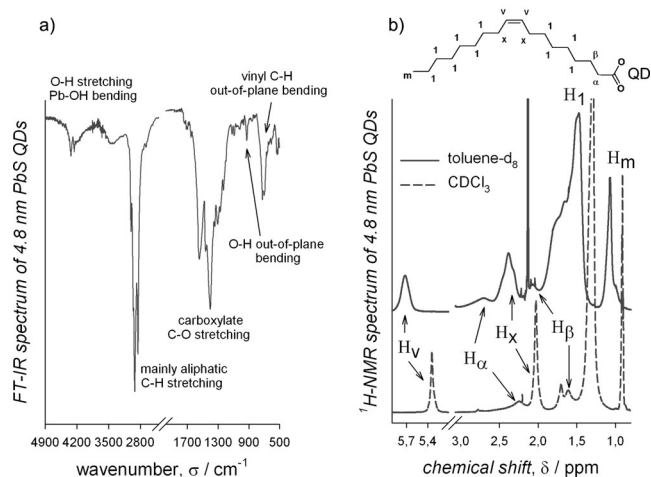


Figure 2. a) FTIR spectrum of PbS QDs with 4.8 nm diameter in the solid phase. b) Atom numbering scheme and ^1H NMR spectra of 0.1 mM N_2 -saturated solutions of colloidal PbS QDs with 4.8 nm diameter in $[\text{D}_8]$ toluene (solid line) and CDCl_3 (dashed line).

a broad weak band at about 3300 cm^{-1} and narrow peaks in the NIR spectral range (above 4000 cm^{-1}) attributed to a combination of Pb–OH stretching modes in analogy with metal hydroxides,^[11] in concomitance with narrow hydroxyl out-of-plane bending modes (at ca. 930 cm^{-1}). The hydroxide anions have been suggested to be derived from water formed upon reaction of PbO with oleic acid.^[12] The FTIR spectrum of the isolated Pb precursor, which was prepared and purified using the same procedure as for QD synthesis yielding a dry white powder that has been clearly identified as Pb-dioleate species (by TGA and ^1H NMR spectroscopy; see Supporting Information), suggests the presence of coordinated water. We argue that coordinated water can protonate an oleate ligand of the Pb-dioleate precursor leading to the release of an oleic acid molecule and leaving behind the Pb(OH) oleate complex (Figure S9). This acid–base equilibrium poses hydroxide anions as plausible QD ligands preserving charge neutrality, although quantification remains elusive from our data. These considerations imply that the presence of PbS nuclei during QD synthesis shifts the equilibrium towards the dissociation of an oleic acid ligand from the Pb dioleate complex. The stereochemical arrangement of two oleate ligands in the Pb precursor may result in marked steric encumbrance, thus promoting the formation of Pb(OH) oleate complexes at the QD surface. Moreover, favorable inter-oleyl hydrophobic interactions involving adjacent Pb complexes at the QD surface may contribute to further stabilize the Pb(OH) oleate ligands. Such inter-oleyl hydrophobic interactions may contribute to broaden the ^1H NMR resonances of PbS QDs in $[\text{D}_8]$ toluene (Figure 2b) as a result of fast ^1H nuclei relaxation. Conversely, the ^1H NMR spectra of PbS QDs recorded in more polar solvents (such as CDCl_3 , Figure 2b) show only slightly broadened resonances of QD-bound oleyl moieties at chemical shifts that coincide with the well-resolved multiplets obtained for the purified Pb precursor (Figure S10), thus suggesting reduced inter-oleyl interactions at the QD surface in polar solvents.

Unambiguous differences are observed for ^1H NMR spectra of QDs of increasing size at the same concentration in $[\text{D}_8]$ toluene (Figure 3a): upon reduction of the QD diameter, the broad oleyl resonances markedly shift upfield and sharpen. These spectral differences cannot be attributed to improper purification because all QD samples exhibit similar oleyl-to- Pb_{exc} ratio and fully Pb-terminated facets. The size-dependent spectral features may instead result from the

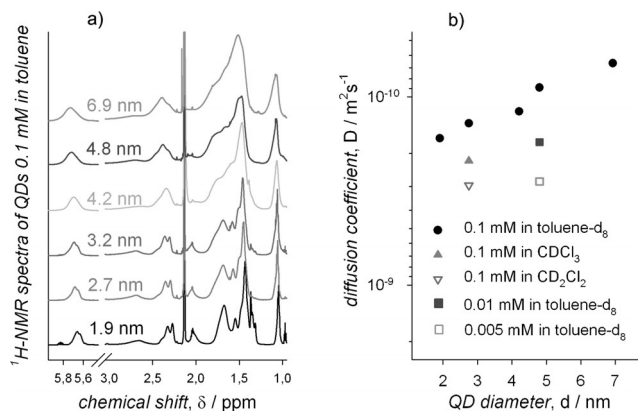


Figure 3. a) ^1H NMR spectra of 0.1 mM $[\text{D}_8]$ toluene N_2 -saturated solutions of colloidal PbS QDs of different sizes. b) Diffusion coefficients as a function of QD size of colloidal PbS QDs in 0.1 mM $[\text{D}_8]$ toluene (filled circles), of PbS QDs with diameter of 2.7 nm in chlorinated solvents (triangles), and of PbS QDs with diameter of 4.8 nm in $[\text{D}_8]$ toluene at lower concentrations (squares).

presence of a larger number of ligands associated with larger QDs, which enhances inter-oleyl interactions thus contributing to peak broadening. The ^1H NMR spectra of QD samples in CDCl_3 show oleyl resonances at chemical shifts that coincide with those of the Pb precursor (Figure S12), which may result from reduced inter-ligand interactions occurring in polar solvents. To understand these size- and medium-dependent spectral features, we performed diffusion ordered NMR spectroscopy (DOSY) measurements on solutions of purified PbS QDs at fixed concentration. In $[\text{D}_8]$ toluene we observed that the QD diffusion coefficient, D , increases with QD size (Figure 3b) yielding solvodynamic radii consistent with the related excitonic diameters (Figure S13). However, oleyl-based ligands at the QD surface in polar solvents (CDCl_3 and CD_2Cl_2 in Figure 3b) seem to diffuse faster than in apolar media. We ascribe the apparent faster diffusion to partial desorption of ligands from the QD surface with an exchange rate that is faster than the DOSY time scale (100 ms), thus yielding D values that are the weighted mean of those of bound and unbound ligands. On this basis and consistent with the previous discussion on inter-ligand interactions, it is thus safe to conclude that increasing solvent polarity promotes partial dissociation of the ligand/core adducts, which implies improved solvation of ligands (and cores) in CDCl_3 and CD_2Cl_2 . Moreover, the diffusion of oleyl moieties in QD samples is markedly affected by concentration (Figure 3b): dilution stabilizes dissociated ligands and cores leading to apparently larger D values, as expected for adducts under thermodynamic equilibrium.

To gain insights into the interfacial dynamics, we perturbed the ligand/core equilibrium by adding to the purified PbS QD solutions the chemical species used in the synthetic procedure that are reasonably expected to constitute the colloidal QD soft surface: namely, the oleic acid reagent and the Pb precursor. Oleic acid addition to 4.8 nm diameter PbS QDs induced a progressive decrease (up to ca. 20 %) of the peak intensities of QD-bound ligands and the appearance of upfield-shifted signals at chemical shifts and with line-widths in between those of bound and free oleic acid (particularly evident for isolated vinylene signals; Figure 4a). It is reasonable to suppose that excess oleic acid molecules coordinate

displaced Pb oleate complexes (Figure S21). Titration experiments conducted in CDCl_3 revealed the reduced stability of the ligand/core adducts compared to in toluene (see Supporting Information).

When adding the Pb precursor to 4.8 nm diameter PbS QDs, the ^1H NMR spectra show the concurrent appearance of narrow upfield-shifted peaks attributed to extra added Pb dioleate, whereas peak intensities of bound oleyl-based ligands are almost unaffected (see Figure 4c). A dynamic interaction between the extra added Pb precursor and the QD surface is suggested by ROESY measurements (Figure 4d). The fast exchange between bound and free Pb oleate species can be explained by the labile character of Pb oleate/core adducts. ^1H NMR titration measurements conducted in CDCl_3 again suggest less-stable ligand/core adducts (see Supporting Information). To substantiate our findings, an analogous set of experiments was carried out by adding oleic acid and the Pb precursor to smaller PbS QDs (with a 2.7 nm diameter) in both $[\text{D}_8]\text{toluene}$ and CDCl_3 solutions yielding qualitatively similar results (Figures S22–26). The rationale for the observed interfacial dynamics may reside in the mutual exchange at the QD surface between oleic acid and Pb oleate, which in turn are indistinguishable by NMR techniques when both species are present, as also evinced from ^1H NMR and DOSY measurements of purified Pb dioleate precursor upon addition of oleic acid molecules (Figures S27–29).

Our studies thus allow a synoptic conceptualization of the dynamic equilibria occurring at the PbS QD surface in solution phase, as depicted in Figure 5.

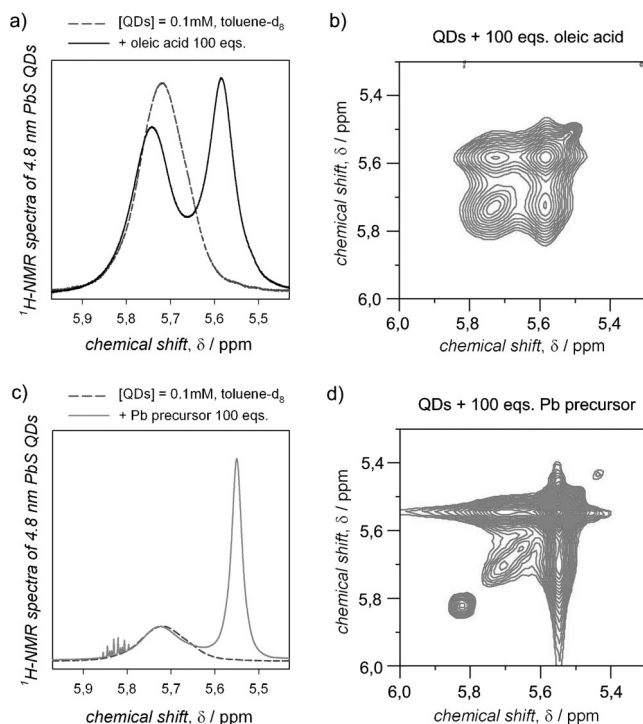


Figure 4. a,c) Vinylene region of the ^1H NMR spectra of PbS QDs with diameter of 4.8 nm in 0.1 mM $[\text{D}_8]\text{toluene}$ N_2 -saturated solutions upon adding 100 equivalents of oleic acid (a) and the Pb precursor (c). b,d) Corresponding ROESY spectra of the same PbS QD solutions upon addition of 100 equivalents of oleic acid (b) and of the Pb precursor (d).

$\text{Pb}(\text{OH})$ oleate ligands inducing their displacement (commonly referred to as Z-type displacement)^[13] predominantly from the {100} facets, which constitute 22.4 % of the surface of a truncated octahedron and which showed lower binding energies for Pb-carboxylate ligands than the {111} facets.^[14] Interfacial dynamics in the presence of excess oleic acid was investigated by DOSY (Figure S14) and nuclear Overhauser effect spectroscopy (NOESY and ROESY; Figure S19) experiments. Two oleyl-based species are resolved in the diffusion domain by DOSY and their resonances show strong and negative NOE contacts with the same (negative) sign of the diagonal peaks, as expected for chemical species in fast exchange (Figure 4b). These findings thus indicate equilibrium mixtures of QD-bound ligands, extra added oleic acid, and

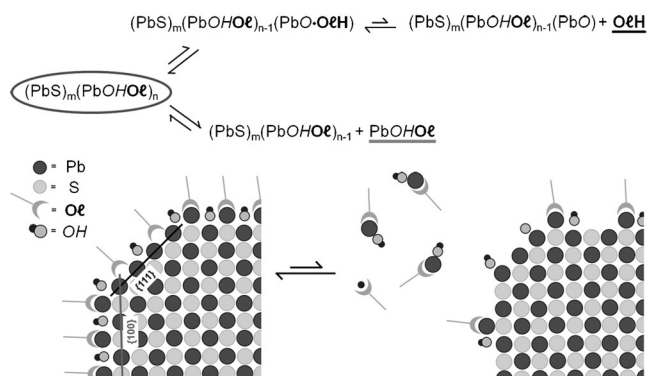


Figure 5. Simplified chemical formula of colloidal PbS QDs and schematic representation of the dynamic equilibria involving oleic acid (O/H) and Pb oleate (PbOHOL) as ligands at the {111} and {100} facets of the QD.

Ligand–ligand and ligand–solvent interactions play a relevant role in determining thermodynamic stability and kinetic lability of the ligand/core adducts. Indeed, the lower stability of ligand/core adducts in polar solvents can be related to the lack of long-term colloidal stability of QDs stored in chlorinated solvents, which are commonly avoided on empirical basis to preserve stable QD dispersions. In this regard, we suggest that highly labile Pb complexes may form when

exchanging pristine oleate ligands for inorganic anions upon phase-transfer to high polarity solvents, such as formamides.^[15] Along with solvent dependence, the low QD concentrations used to determine ensemble photoluminescence quantum yields (ca. μM , usually) may affect the measured values as a result of the dynamic formation of in-gap states related to the equilibrium surface chemistry of colloidal QDs; relevance to photoluminescence blinking and spectral diffusion is consequently envisaged (samples for single QD measurements are prepared from sub-nM solutions). By extension, the QD surface may also be perturbed in the solid-state by nuclear rearrangement upon excitation light absorption and/or charge injection that operate QD-based optoelectronic devices.

We foresee a potential general validity for the dynamic equilibria at the surface of colloidal metal chalcogenide QDs, although with a marked dependence on the specific ligand/core adducts under consideration. CdSe QDs capped with (Cd-)oleate ligands showed solvent-dependent ^1H NMR spectra and an inferred labile character of ligands,^[7] in analogy to the PbS QDs discussed herein, although addition of oleic acid was reported not to induce Cd oleate displacement from CdSe QD surface.^[16] Discrepancies between interfacial dynamics of Cd and Pb chalcogenide QDs could find an explanation in the different electronic configuration of the metal cations, with Pb^{II} showing 6s electron lone pairs that can be stereochemically active hence significantly reducing the stability (and also increasing lability) of Pb oleate coordination to the PbS crystallite surface. Our findings may also contribute to explaining some of the most common synthetic procedures used to tune the size of metal chalcogenide QDs:^[8,17] the mutual exchange involving excess oleic acid and metal dioleate complex(es) reduces the reactivity of the metal precursors, therefore fewer nuclei and consequently larger QDs are obtained upon increasing the concentration of oleic acid in weakly coordinating solvents, for given time and temperature of the reaction.

More broadly, we note the hybrid organic/inorganic character of colloidal QDs and the importance of conceiving them as inherently dynamic chemical species rather than as discrete entities, thus showing equilibrium structures that largely depend on the QD's surroundings. The ligand/core dynamic equilibrium may have relevant implications for the design of novel synthetic paths by tuning the affinity of reaction precursors for specific QD facets during nanocrystal growth. In addition, this notion can prompt refined (asymmetric) post-synthesis QD surface chemical modification procedures in the solution-phase by suggesting the exchange of native ligands under thermodynamic control, to ultimately yield defect-free conductive QD solids for efficient (opto-)electronic applications.

Acknowledgements

We thank L. Carbone, I. Infante, and R. Giannuzzi for fruitful discussion and R. Di Corato and A. Fiore for technical assistance. This work was supported by Progetto di ricerca PON R&C 2007-2013 MAAT (no: PON02_00563_3316357).

C.G. thanks the "Future In Research" program by Regione Puglia (code: ZCZP7C3).

Keywords: colloidal quantum dots · coordination chemistry · dynamic equilibrium · ligands · surface chemistry

How to cite: *Angew. Chem. Int. Ed.* **2016**, *55*, 6628–6633
Angew. Chem. **2016**, *128*, 6740–6745

- [1] Y. Yin, A. P. Alivisatos, *Nature* **2005**, *437*, 664–670.
- [2] a) K. Katsiev, A. H. Ip, A. Fischer, I. Tanabe, X. Zhang, A. R. Kirmani, O. Voznyy, L. R. Rollny, K. W. Chou, S. M. Thon, G. H. Carey, X. Cui, A. Amassian, P. Dowben, E. H. Sargent, O. M. Bakr, *Adv. Mater.* **2014**, *26*, 937–942; b) P. R. Brown, D. Kim, R. R. Lunt, N. Zhao, M. G. Bawendi, J. C. Grossman, V. Bulović, *ACS Nano* **2014**, *8*, 5863–5872; c) C. Giansante, I. Infante, E. Fabiano, R. Grisorio, G. P. Suranna, G. Gigli, *J. Am. Chem. Soc.* **2015**, *137*, 1875–1886.
- [3] a) J. J. Choi, C. R. Bealing, K. Bian, K. J. Hughes, W. Zhang, D.-M. Smilgies, R. G. Hennig, J. R. Engstrom, T. Hanrath, *J. Am. Chem. Soc.* **2011**, *133*, 3131–3138; b) C. Giansante, L. Carbone, C. Giannini, D. Altamura, Z. Ameer, G. Maruccio, A. Loiudice, M. R. Belviso, P. D. Cozzoli, A. Rizzo, G. Gigli, *J. Phys. Chem. C* **2013**, *117*, 13305–13317; c) R. Li, K. Bian, T. Hanrath, W. A. Bassett, Z. Wang, *J. Am. Chem. Soc.* **2014**, *136*, 12047–12055; d) A. C. Balazs, T. Emrick, T. P. Russell, *Science* **2006**, *314*, 1107–1110; e) Y. Li, P. Tao, A. Viswanath, B. C. Benicewicz, L. S. Schadler, *Langmuir* **2013**, *29*, 1211–1220; f) C. Giansante, R. Mastria, G. Lerario, L. Moretti, I. Kriegel, F. Scotognella, G. Lanzani, S. Carallo, M. Esposito, M. Biasucci, A. Rizzo, G. Gigli, *Adv. Funct. Mater.* **2015**, *25*, 111–119.
- [4] a) L. Manna, E. C. Scher, A. P. Alivisatos, *J. Am. Chem. Soc.* **2000**, *122*, 12700–12706; b) K.-S. Cho, D. V. Talapin, W. Gaschler, C. B. Murray, *J. Am. Chem. Soc.* **2005**, *127*, 7140–7147; c) J. M. Pietryga, D. J. Werder, D. J. Williams, J. L. Casson, R. D. Schaller, V. I. Klimov, J. A. Hollingsworth, *J. Am. Chem. Soc.* **2008**, *130*, 4879–4885.
- [5] a) I. L. Medintz, H. T. Uyeda, E. R. Goldman, H. Mattoussi, *Nat. Mater.* **2005**, *4*, 435–446; b) D. V. Talapin, J.-S. Lee, M. V. Kovalenko, E. V. Shevchenko, *Chem. Rev.* **2010**, *110*, 389–458; c) Y. Shirasaki, G. J. Supran, M. G. Bawendi, V. Bulovic, *Nat. Photonics* **2013**, *7*, 13–23.
- [6] a) X. Ji, D. Copenhaver, C. Sichel, X. Peng, *J. Am. Chem. Soc.* **2008**, *130*, 5726–5735; b) A. Hassinen, I. Moreels, C. de Mello Donegá, J. C. Martins, Z. Hens, *J. Phys. Chem. Lett.* **2010**, *1*, 2577–2581.
- [7] N. C. Anderson, M. P. Hendricks, J. J. Choi, J. S. Owen, *J. Am. Chem. Soc.* **2013**, *135*, 18536–18548.
- [8] M. A. Hines, G. D. Scholes, *Adv. Mater.* **2003**, *15*, 1844–1849.
- [9] A. Hassinen, I. Moreels, K. De Nolf, P. F. Smet, J. C. Martins, Z. Hens, *J. Am. Chem. Soc.* **2012**, *134*, 20705–20712.
- [10] a) I. Moreels, B. Fritzing, J. C. Martins, Z. Hens, *J. Am. Chem. Soc.* **2008**, *130*, 15081–15086; b) B. K. Hughes, D. A. Ruddy, J. L. Blackburn, D. K. Smith, M. R. Bergren, A. J. Nozik, J. C. Johnson, M. C. Beard, *ACS Nano* **2012**, *6*, 5498–5506; c) H. Choi, J.-H. Ko, Y.-H. Kim, S. Jeong, *J. Am. Chem. Soc.* **2013**, *135*, 5278–5281.
- [11] R. N. Clark, T. V. V. King, M. Klejwa, G. A. Swayze, N. Vergo, *J. Geophys. Res.* **1990**, *95*, 12653–12680.
- [12] D. Zhrebetskyy, M. Scheele, Y. Zhang, N. Bronstein, C. Thompson, D. Britt, M. Salmeron, P. Alivisatos, L.-W. Wang, *Science* **2014**, *344*, 1380–1384.
- [13] M. L. H. Green, *J. Organomet. Chem.* **1995**, *500*, 127–148.
- [14] a) C. R. Bealing, W. J. Baumgardner, J. J. Choi, T. Hanrath, R. G. Hennig, *ACS Nano* **2012**, *6*, 2118–2127; b) J. Y. Woo, J.-H. Ko, J. H. Song, K. Kim, H. Choi, Y.-H. Kim, D. C. Lee, S. Jeong, *J.*

- Am. Chem. Soc.* **2014**, *136*, 8883–8886; c) C. S. S. Sandeep, J. M. Azpiroz, W. H. Evers, S. C. Boheme, I. Moreels, S. Kinge, L. D. A. Siebbeles, I. Infante, A. J. Houtepen, *ACS Nano* **2014**, *8*, 11499–11511.
- [15] a) M. V. Kovalenko, M. I. Bodnarchuk, J. Zaumseil, J.-S. Lee, D. V. Talapin, *J. Am. Chem. Soc.* **2010**, *132*, 10085–10092; b) S. Kim, J. Noh, H. Choi, H. Ha, J. H. Song, H. C. Shim, J. Jang, M. C. Beard, S. Jeong, *J. Phys. Chem. Lett.* **2014**, *5*, 4002–4007; c) S. E. Doris, J. J. Lynch, C. Li, A. W. Wills, J. J. Urban, B. A. Helms, *J. Am. Chem. Soc.* **2014**, *136*, 15702–15710.
- [16] B. Fritzing, R. K. Capek, K. Lambert, J. C. Martins, Z. Hens, *J. Am. Chem. Soc.* **2010**, *132*, 10195–10201.
- [17] a) W. W. Yu, X. Peng, *Angew. Chem. Int. Ed.* **2002**, *41*, 2368–2371; *Angew. Chem.* **2002**, *114*, 2474–2477; b) S. Abe, R. K. Capek, B. De Geyter, Z. Hens, *ACS Nano* **2013**, *7*, 943–949.

Received: December 4, 2015

Revised: February 19, 2016

Published online: April 1, 2016